Asian Journal of Green Chemistry 10 (2026) 673-693

Asian Journal of Green Chemistry

Original Research Article View Article Online | View Journal

A Novel Biosorbent Derived from Matoa Seeds (*Pometia pinnata*) for Lead Removal: Optimization and Material Characterization

Arief Yandra Putra [1,2], Safni Safni[1,*], Rahmiana Zein[1], Emriadi Emriadi[1]

[1]*Department of Chemistry, Faculty of Mathematics and Natural Sciences, Andalas University, Padang, Indonesia*
[2]*Education of Chemistry, Faculty of Teacher Training and Education, Universitas Islam Riau, Pekanbaru, Indonesia*

ARTICLE INFORMATION

Submitted: 2025-11-16
Revised: 2026-01-01
Accepted: 2026-02-02
Published: 2026-02-04
Manuscript ID: AJGC-2512-1892
DOI: 10.48309/AJGC.2026.566613.1892

KEYWORDS

Pb(II) removal
Matoa seeds
Biosorbent
RSM-BBD

ABSTRACT

Heavy metal pollution, particularly Pb(II), remains a primary environmental and public health concern due to its persistence and toxicity. This work evaluates the potential of matoa seed (*Pometia pinnata*) seed powder as an inexpensive and sustainable biosorbent for removing Pb(II) from aqueous systems. Before application, the material was chemically activated and examined using Fourier transform infrared spectroscopy (FTIR), scanning electron microscopy with energy dispersive X-ray (SEM–EDX) analysis, Brunauer–Emmett–Teller (BET) analysis, and X-ray fluorescence (XRF) analysis to elucidate its structural and surface characteristics. The adsorption variables pH, initial Pb(II) concentration, and contact time were optimized through response surface methodology (RSM) employing a Box–Behnken design (BBD). The optimum conditions were achieved at a pH of 6, an initial metal concentration of 600 mg/L, and a contact time of 60 min, yielding an adsorption capacity of 74 mg/g. Statistical evaluation revealed that the initial ion concentration and the quadratic term in contact time significantly influenced Pb(II) uptake. Spectral analysis confirmed the presence of oxygen-containing functional groups, while morphological and elemental examinations verified the accumulation of Pb on the biosorbent surface. These findings highlight matoa seed powder as a promising natural material for Pb(II) remediation and demonstrate the applicability of RSM for optimizing biosorption processes.

Corresponding author, E-mail: safni@sci.unand.ac.id (S. Safni)
Tel.: +081374282673

Graphical Abstract

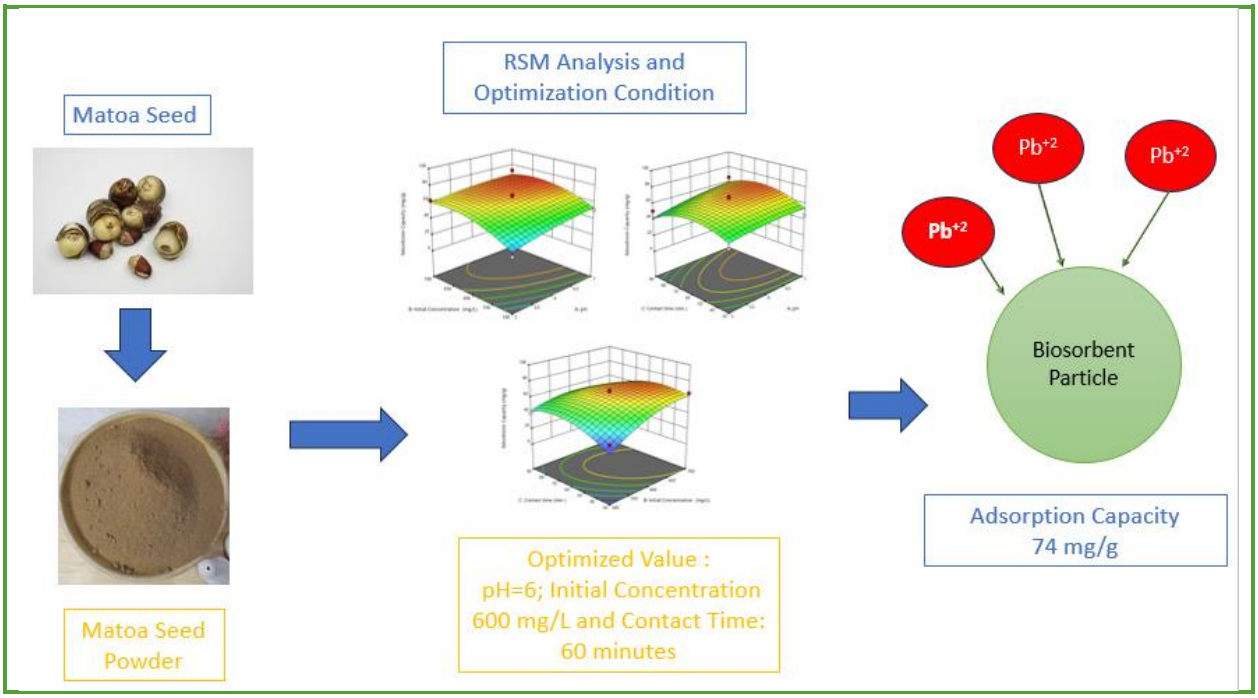

Introduction

The rapid industrial development aimed at meeting increasing human needs has intensified environmental pressures [1]. As industries expand, they generate substantial amounts of liquid and solid waste as byproducts of various processes, contributing significantly to environmental degradation [2]. Among these pollutants, heavy metal contamination has become a significant global concern. Heavy metals are commonly classified according to their density or, from a physical perspective, by their atomic number. Although some of these metals play essential roles in biological systems at trace levels, excessive exposure can disrupt vital physiological functions. Prolonged or elevated intake of heavy metals may lead to severe toxic effects, including organ damage, neurological disorders, and, in extreme cases, fatal outcomes. Their harmful impact can extend to multiple organs, including the skin, respiratory tract, digestive system, kidneys, liver, and cardiovascular tissues. While not all heavy metals are inherently hazardous, they become harmful when present at high concentrations or in specific chemical forms that increase their reactivity [3]. Heavy metals can be removed from wastewater using various treatment technologies, including chemical precipitation, coagulation, flocculation, ion exchange, and adsorption. However, the widespread use of these conventional methods is often constrained by inherent drawbacks, including the production of sludge enriched with toxic metals and the relatively high operational costs associated with their application [4]. Biosorption has emerged as an alternative approach within physicochemical treatment strategies, relying on non-living biological materials rather than active microbial metabolism [5]. This technique is valued for its affordability, operational simplicity, and high removal efficiency, making it a reliable option for treating metal-contaminated water [6]. The biosorption mechanism typically involves two

interacting phases: a solid biosorbent, commonly derived from plant residues, activated carbon, or other biomass, and a liquid phase containing dissolved metal ions, known as the sorbate. Agricultural byproducts, bacterial biomass, and fungal materials have been widely explored as biosorbents due to their abundance of functional groups, including carbonyl, carboxyl, phenolic, and amine groups, which enable effective binding of both cationic and anionic species [5, 7].

In recent years, matoa seeds (*Pometia pinnata*) have gained popularity in Riau Province, Indonesia, primarily due to their appealing fruit, which offers a unique flavor profile reminiscent of a blend of rambutan, longan, and durian [8]. In addition to their nutritional value, matoa leaves contain various antioxidant compounds, including epicatechin, kaempferol-3-*O*-rhamnoside, quercetin-3-O-rhamnoside, glycolipids, steroid glycosides, stigmasterol-3-O-glucoside, and pentacyclic triterpenoid saponins [3-*O*-*α*-arabinofuranosyl-(1→3)-*α*-rhamnopyranose-(1→2)-*α*-arabinopyranose hederagenin]. The hepatoprotective potential associated with matoa leaves is linked to their rich antioxidant components. Additionally, the potent antioxidant activity of matoa peel enhances its potential as a natural source of antioxidant compounds [9]. The carbon composition of activated carbon derived from matoa was found to be around 99.21% by SEM–EDX analysis. This material demonstrated effective adsorption of Cd(II) under alkaline conditions (pH 9), yielding optimal performance after a 40 min contact time with an initial concentration of 20 mg/L. Activated carbon produced from matoa fruit peel and modified with nitric acid exhibited an adsorption capacity of 59.75 mg/g [10]. The purpose of this study is to evaluate the potential of *Pometia pinnata* seeds as an adsorbent for Pb(II) removal using a batch adsorption system based on these findings. The key novelty of this work lies in the application of matoa seeds (*Pometia pinnata*), previously unexplored for heavy metal remediation, as a biosorbent for Pb(II) adsorption under practically relevant conditions. This is the first study demonstrating the use of matoa seed-based biosorbents for Pb(II) removal, achieving effective adsorption at near-neutral pH and relatively high initial metal concentrations.

Experimental

Material

Matoa fruit seeds (*Pometia pinnata*) were collected from Pekanbaru, Riau, Indonesia. All chemicals, including potassium dichromate ($K_2Cr_2O_7$), nitric acid (HNO_3), sodium hydroxide (NaOH), and a buffer solution (pH 2–6), were supplied by Merck as analytical grade. All reagents were dissolved in distilled water.

Method

Bioadsorbent preparation and characterization

Matoa seeds were washed, air dried, and ground into a powder before being sieved to obtain a uniform particle size (36 mesh). The powder was subjected to acid activation by soaking in HNO_3 for 120 min. After activation, the material was repeatedly rinsed with distilled water until the filtrate reached neutral pH, followed by drying at 80 °C for 60 min. The dried sample was stored in a desiccator prior to use. FTIR, SEM–EDX, BET, and XRF analyses were conducted to assess functional groups, surface morphology, pore characteristics, and elemental composition, respectively [11].

Point zero charge (pHpzc) adsorption study

The preparation of 0.1 M KCl solutions with initial pH values ranging from 2 to 7 involved

adjustments with dilute HNO_3 or NaOH. Approximately 0.1 g of the biosorbent was added to 25 mL of each solution and agitated at 100 rpm for 24 h. Changes in pH before and after equilibrium were recorded, and the pHpzc was determined from the intersection point where ΔpH equals zero [12].

Adsorbent characterization

The characterization of the adsorbent was carried out by FTIR (Unican Mattson Mod 7000 FTIR, SEM-EDX (Hitachi S-3400N), BET (Quantachrome Nova 4200e), and XRF (PANalytical epsilon 3).

Biosorption experiment

The adsorption experiments were conducted by introducing 0.1 g of finely powdered matoa seed biosorbent (particle size ≤ 36 μm) into a 10 mL Pb(II) solution contained in a 25 mL Erlenmeyer flask. The suspensions were then shaken at 100 rpm to ensure proper mixing. The pH of each solution was adjusted to the required value (2–6) using dilute HNO_3 or NaOH. A series of operating conditions was systematically explored, including variations in pH (2–6), initial Pb(II) concentrations (100–1,000 mg/L), contact times (15–90 min), and temperatures (298–318 K). For optimization purposes, pH, initial metal concentration, and contact time were selected as the independent factors, while adsorption capacity (mg/g) served as the response variable. Optimization of the process parameters was performed using Response Surface Methodology based on a Box–Behnken Design (RSM–BBD), incorporating the three selected factors. Data processing and model development were conducted using Design Expert version 13. Concentrations of Pb(II) before and after adsorption were quantified using an atomic absorption spectrophotometer (AAS) (AA240) operating at 429 nm. The removal efficiency and adsorption capacity of Pb(II) were calculated using Equations 1 and 2, respectively.

$$\text{Adsorption efficiency (\%R)} = \frac{(Co - Ce)}{Co} \times 100\% \quad (1)$$

$$\text{Adsorption capacity (q)} = \frac{(Co - Ce)V}{m} \quad (2)$$

Where. Co and Ce (mg/L) are the initial and equilibrium concentrations of Pb(II), respectively, V (L) is the volume of the solution, and m (g) is the mass of the biosorbent used [11].

The experimental factors and their corresponding levels used in the Box–Behnken Design are summarized in Table 1.

Table 1. The independent variables consisted of three key factors, which were evaluated using the response surface methodology based on a BBD.

Independent variables	Low	Center	High
pH	3	5	7
Initial concentration Pb(II) (mg/L)	500	600	700
Contact time (min)	30	60	90

Results and Discussion

Determination of the point of zero charge (pH pzc)

The point of zero charge (pHpzc) represents the pH at which the adsorbent's surface carries no net electrical charge, meaning that the proportions of positive and negative surface sites are equal. In graphical form, this condition corresponds to the point where the ΔpH curve crosses the X-axis. The pHpzc is an important indicator of how the material interacts with ionic species in solution. When the solution pH exceeds the pHpzc, the surface becomes predominantly negatively charged, thereby promoting the adsorption of cationic metal ions. In contrast, at pH values below the pHpzc, the surface develops a net positive charge, which

favors the attraction and binding of anionic species [5].

Figure 1 shows that the curve of ΔpH versus initial pH intersects at approximately pH 4.1, representing the pHpzc of the material. At this point, the surface carries no net charge and does not preferentially attract or release protons. When the solution pH falls below 4.1, the surface becomes positively charged, which enhances its affinity for anionic species such as CrO_4^{2-} or NO_3^-. In contrast, at pH values above 4.1, the surface develops a negative charge, making it highly effective for binding cationic species, including heavy metal ions like Pb(II). Therefore, operating at pH values greater than 4.1 is advantageous for Pb(II) removal, as the negatively charged surface promotes stronger electrostatic attraction and facilitates greater uptake of Pb(II) ions, ultimately improving the overall efficiency of the adsorption process in aqueous systems.

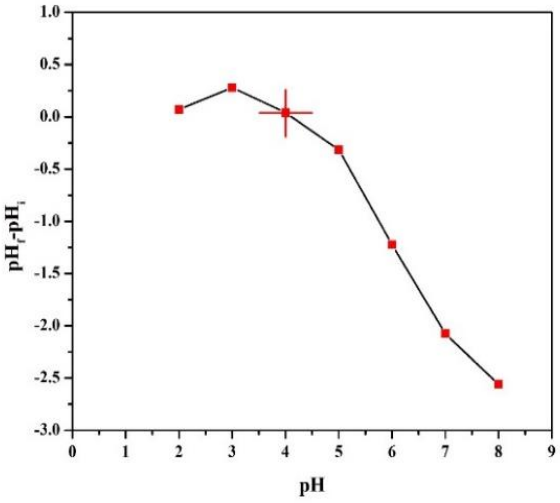

Figure 1. pH value of pzc from matoa seeds

Effect of solution pH

Figure 2 shows that the highest adsorption capacity for Pb(II) is achieved at pH 6, reaching approximately 11,200 mg/g. This suggests that both the surface chemistry of the adsorbent and the predominant Pb species present at this pH create optimal conditions for metal uptake. At more acidic conditions, such as pH 3, the abundance of H^+ ions competes with Pb(II) for the available binding sites, reducing adsorption performance. Conversely, at pH values around 7, the potential formation of $Pb(OH)_2$ decreases the amount of free Pb(II) in solution, thereby lowering the effective adsorption. These observations align with the results of Mashentseva *et al.*, who reported that biogenic metal oxide nanoparticles (ZnO and CuO) exhibited maximum adsorption within a pH range of 5.5–6, following pseudo-second-order kinetics and the Freundlich isotherm [13]. Likewise, Zhang *et al.*, found that the prepared adsorbent achieved rapid and efficient removal of Pb(II) and Cd(II), with peak adsorption occurring at pH 6 [14]. Collectively, these findings reinforce that pH 6 represents the optimum condition for Pb(II) adsorption.

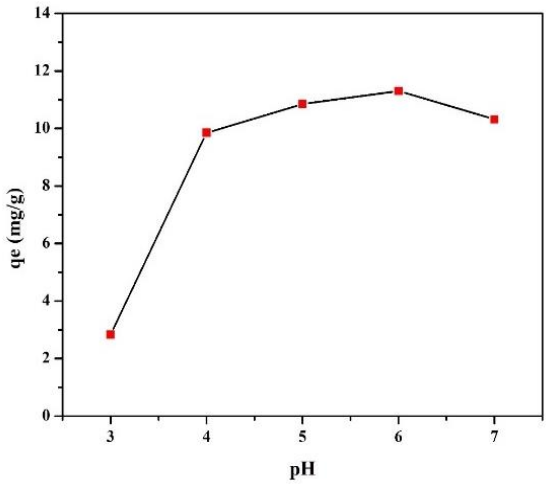

Figure 2. Optimal pH for Pb(II) adsorption using matoa seed biosorbent

Effect of initial concentration

Figure 3 illustrates that the adsorption capacity increases with the initial Pb(II) concentration, reaching a maximum of 73 mg/g at 600 mg/L before declining at higher concentrations. The initial increase is attributed to the greater abundance of Pb(II) ions in solution, which enhances their diffusion toward and interaction with the available active sites on the adsorbent. Once these sites become saturated, however, additional ions compete for limited binding locations, resulting in a decrease in adsorption efficiency. These findings can be compared with those reported for a cellulose hydrogel, which achieved a much higher maximum adsorption capacity of 486 mg/g at initial concentrations of 400–500 mg/L. The superior performance of the hydrogel is attributed to its extensive pore network and abundance of functional groups, which facilitate metal uptake, as well as its ability to undergo up to eight regeneration cycles with efficiencies exceeding 79% [15].

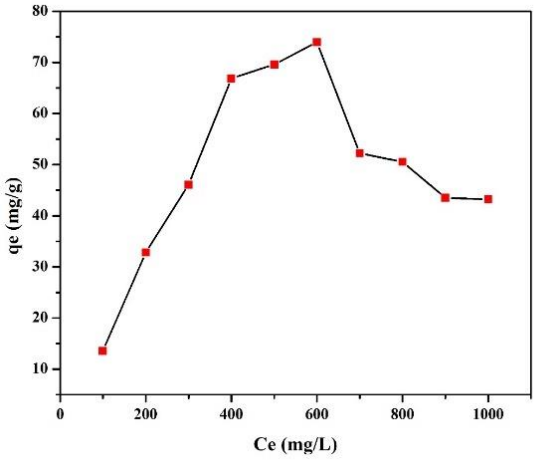

Figure 3. Effect of initial concentration on Pb(II) adsorption by matoa seed biosorbent

Conversely, a study employing natural red earth as an adsorbent reported a significantly lower maximum capacity of 10.31 mg/g at an initial concentration of 100 mg/L. The reduced performance of red earth is attributed to its limited surface area and fewer active binding sites, resulting in an earlier saturation point and substantially lower adsorption capability compared to engineered or functionalized adsorbents [16].

Effect of contact time

Figure 4 shows that the adsorption capacity of Pb(II) ions increases with contact time and reaches its maximum value of 74 mg/g at 60 min. This indicates that by this point, most of the active binding sites on the biosorbent have been occupied by Pb(II) ions, resulting in the highest adsorption performance. At shorter contact times, such as 30 or 45 min, the lower capacity suggests that the diffusion of Pb(II) ions toward the adsorbent surface and their subsequent attachment to active sites are still incomplete. Experiencing more than 60 min, the adsorption capacity declines steadily at 90, 120, and 150 min. This reduction may be associated with partial desorption of bound Pb(II) ions, saturation of available sites, or increased competition among ions for limited binding locations. Prolonged interaction may also alter the surface characteristics of the biosorbent, thereby contributing to a decrease in efficiency.

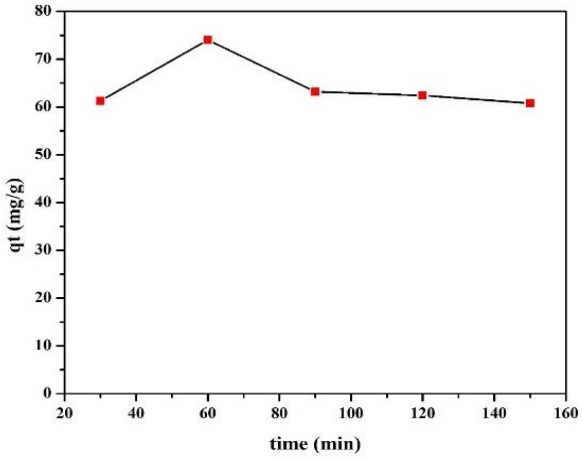

Figure 4. Effect of contact time on Pb(II) adsorption by matoa seed biosorbent

These observations align with findings reported by Ali, who noted an optimal contact time of 45 min for Pb(II) removal, after which the system approached equilibrium, and further improvement was minimal [17]. Likewise, according to Sari *et al*., identified 60 min is the optimal duration, with adsorption efficiency decreasing at later time points. Overall, these results emphasize that saturation of active sites naturally limits adsorption capacity. Contact time is a key operational parameter in developing effective heavy metal removal processes [18].

Effect of temperature

Figure 5 illustrates the relationship between the initial Pb(II) concentration (Co, mg/L) and the equilibrium adsorption capacity (Qe, mg/g) at three temperatures: 298 K, 308 K, and 318 K. The data indicate that the combined effect of temperature and initial metal concentration has a strong influence on the adsorption performance. At lower Co values (10–20 mg/L), the highest Qe is observed at 298 K, suggesting that adsorption is more favorable at lower temperatures when Pb(II) availability is limited.

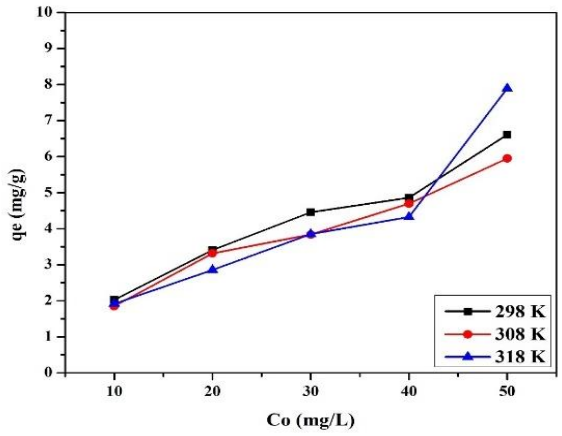

Figure 5. Effect of temperature variation on Pb(II) adsorption

This enhanced performance may be attributed to more stable interactions between Pb(II) ions and surface functional groups, which are less susceptible to thermal agitation. As the concentration increases to intermediate levels (30–40 mg/L), the adsorption capacities at the three temperatures become more comparable, although 298 K still shows a slight advantage.

In contrast, at the highest Co value tested (50 mg/L), a notable rise in Qe is observed at 318 K. This shift suggests that at high ion concentrations, increased thermal energy facilitates the faster diffusion of Pb(II) ions toward the adsorbent and enhances their binding affinity to the active sites. Elevated temperature under these conditions, therefore, contributes to a more efficient adsorption process. These results indicate that the optimal temperature for Pb(II) adsorption varies with the initial metal concentration. At low to moderate concentrations, 298 K provides the highest adsorption efficiency, whereas at elevated concentrations, 318 K yields the best Qe values. This trend agrees with findings reported by Chowdhury *et al*., who observed that increasing temperature enhances the mobility of Pb(II) ions and strengthens their interaction with adsorption sites, particularly when the metal ion concentration is high. Although ambient temperature is often regarded as sufficient for effective adsorption, the observed improvement in Qe at elevated temperatures supports the endothermic character of the process and suggests that higher temperatures promote faster adsorption kinetics [19]. Similarly, Yang *et al.* demonstrated that temperature has minimal influence on Qe at low to intermediate Pb(II) concentrations, with adsorption remaining relatively constant across the temperature range studied. However, at higher concentrations, a noticeable improvement in adsorption capacity was reported. This is consistent with the present

data, which show a substantial increase in Qe at 318 K when Co reaches 50 mg/L, indicating that elevated temperatures facilitate greater diffusion and stronger interaction between Pb(II) ions and the adsorbent surface under high ionic load conditions [20].

Characterization of matoa seeds

FTIR analysis

Figure 6 shows that the FTIR spectra of the biosorbent exhibit notable changes after interaction with Pb(II) ions. Before adsorption, a distinct peak appeared at 2,349.34 cm^{-1}, corresponding to the presence of an O=C=O functional group, which may originate from adsorbed CO_2 or free carboxylate species. This peak is absent in the spectrum following Pb exposure, suggesting that the group either participated in binding with Pb(II) or was removed during the adsorption process. Moreover, the prominent adsorption bands at 2,848.91 and 2,919.31 cm^{-1}, typically associated with C–H stretching vibrations, showed a substantial reduction in intensity after Pb treatment. Only a faint peak near 2,916.42 cm^{-1} remained, indicating that hydrocarbon chains may have been altered or that Pb(II) ions interacted with alkyl groups on the biosorbent surface.

The absorption bands at 1,539.22 and 1,653 cm^{-1}, typically attributed to aromatic C=C stretching or amide-related vibrations, were observed in both the untreated and Pb-loaded biosorbent. However, after adsorption, these peaks exhibited increases in intensity and noticeable changes in peak area, indicating that aromatic rings or peptide-like structures may participate in coordinating Pb(II) ions. Following exposure to Pb(II), a broad band emerged at 3,395.74 cm^{-1}, which was absent in the original spectrum. This feature corresponds to O–H stretching vibrations, suggesting the involvement of hydroxyl groups in metal binding, possibly through hydrogen bonding, polar interactions, hydrolysis, or the formation of new complexed species during adsorption. These results are consistent with those of Li *et al*., who demonstrated that hydroxyl and carboxyl groups in konjac starch-derived biochar play dominant roles in Pb(II) adsorption through complexation and ion exchange mechanisms. Their FTIR spectra likewise showed changes in peak intensity and position after metal uptake, confirming interactions between Pb(II) and surface functional groups [21]. Similarly, Chowdury *et al*. reported a shift

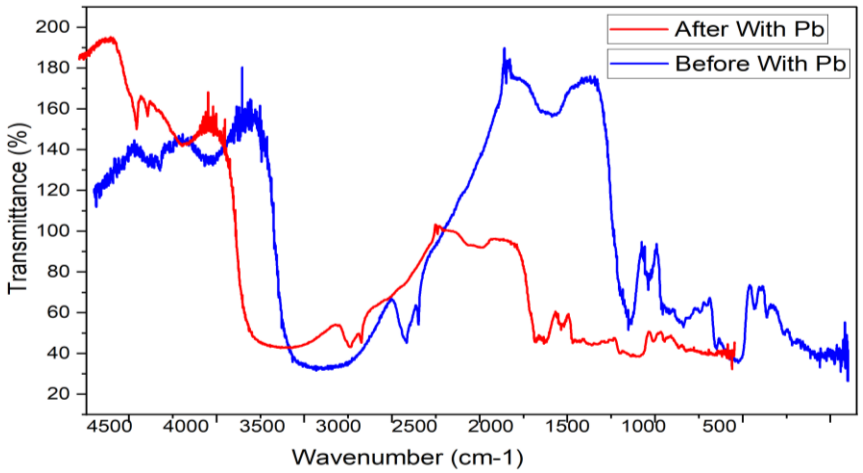

Figure 6. FTIR analysis of the biosorbent before and after Pb(II) absorption

in the O–H stretching region (3,417 → 3,404 cm^{-1}) when using a GO/MIL-53(Al) nanocomposite, further supporting the participation of hydroxyl functionalities in Pb(II) binding [19]. A study by Tang *et al.*, using biochar modified with iron and manganese oxides, also revealed spectral changes at 3434, 2922, 1625, 1,385, and 1,072 cm^{-1}, associated with alterations in hydroxyl, methylene, carbonyl, and carboxyl groups upon interaction with Pb(II).

These shifts collectively illustrate how multiple functional groups contribute to the absorption mechanism [22]. Overall, the comparative studies confirm that variations in FTIR peak intensity and position after metal exposure provide strong evidence of chemical interactions between functional groups on the adsorbent and heavy metal ions. They also highlight that tailoring or enhancing these functional groups can significantly improve the adsorption performance of biosorbents in aqueous environments.

BET analysis

Figure 7 illustrates noticeable alterations in the surface properties of the material following Pb (II) adsorption. The increase in adsorption volume after metal uptake suggests enhanced interactions between Pb(II) ions and the available active sites, which may contribute to changes in surface porosity. Despite this, BET analysis indicates that the specific surface area decreased only slightly from 0.801 to 0.800 m^2/g after adsorption. This minimal change implies that the adsorption of Pb(II) ions did not substantially disrupt or block the pore structure of the material. The preservation of pore integrity demonstrates that the biosorbent maintains structural stability throughout the adsorption process, highlighting its suitability for Pb removal in aqueous systems. This observation aligns with the findings of Chen, who reported that $FeCl_3$ modification of biochar substantially enhanced its textural properties, increasing the specific surface area from 740.012 to 820.504 m^2/g and enlarging the total pore volume from 0.317 to 0.503 cm^3/g [23]. A similar

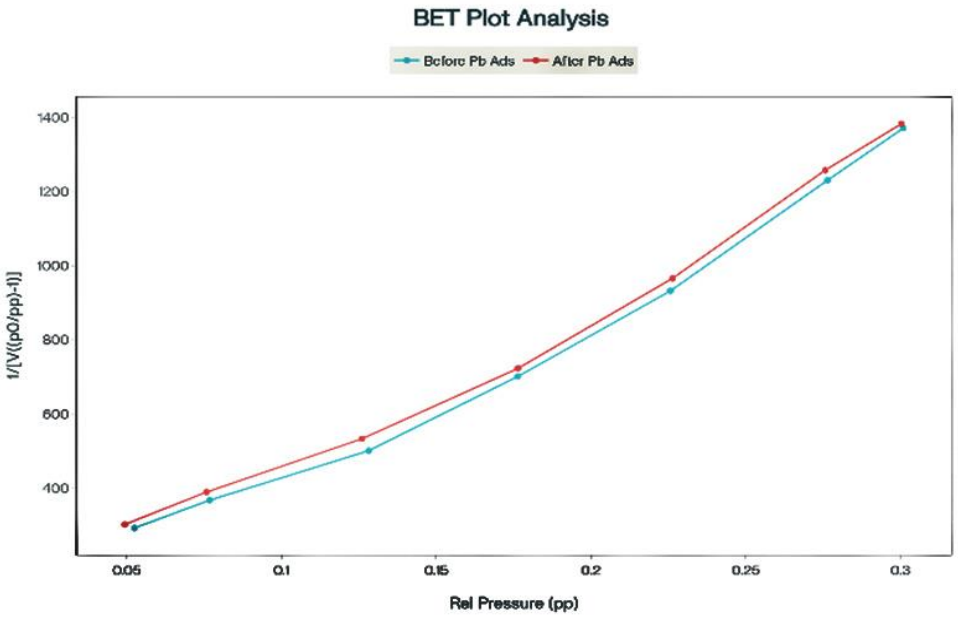

Figure 7. BET analysis before and after Pb(II) adsorption

trend was observed by Yumeng Wu *et al*., who utilized hydrothermally carbonized banana peel and further activated it with KOH for Pb(II) adsorption. BET analysis confirmed that the modification improved both surface area and porosity, contributing to an adsorption capacity of 42.92 mg/g and a removal efficiency of 86.84% [24]. Likewise, Dima Khater investigated activated carbon produced from oak cupules for the removal of several heavy metal ions, including Pb(II). BET characterization revealed that the resulting carbon possessed a notably high surface area, which accounted for its strong adsorption performance [25].

SEM-EDX analysis

Based on Figure 8, the results of the SEM-EDX analysis indicate that the interaction between the sample surface and Pb(II) ions leads to morphological changes, including increased surface roughness, the formation of new particles, and alterations in the chemical composition of the material's surface. The emergence of Pb peaks in the EDX spectrum provides strong evidence that the adsorption of Pb(II) ions successfully occurred on the sample surface. Similar observations have been reported in previous studies by [19,26,27], all of

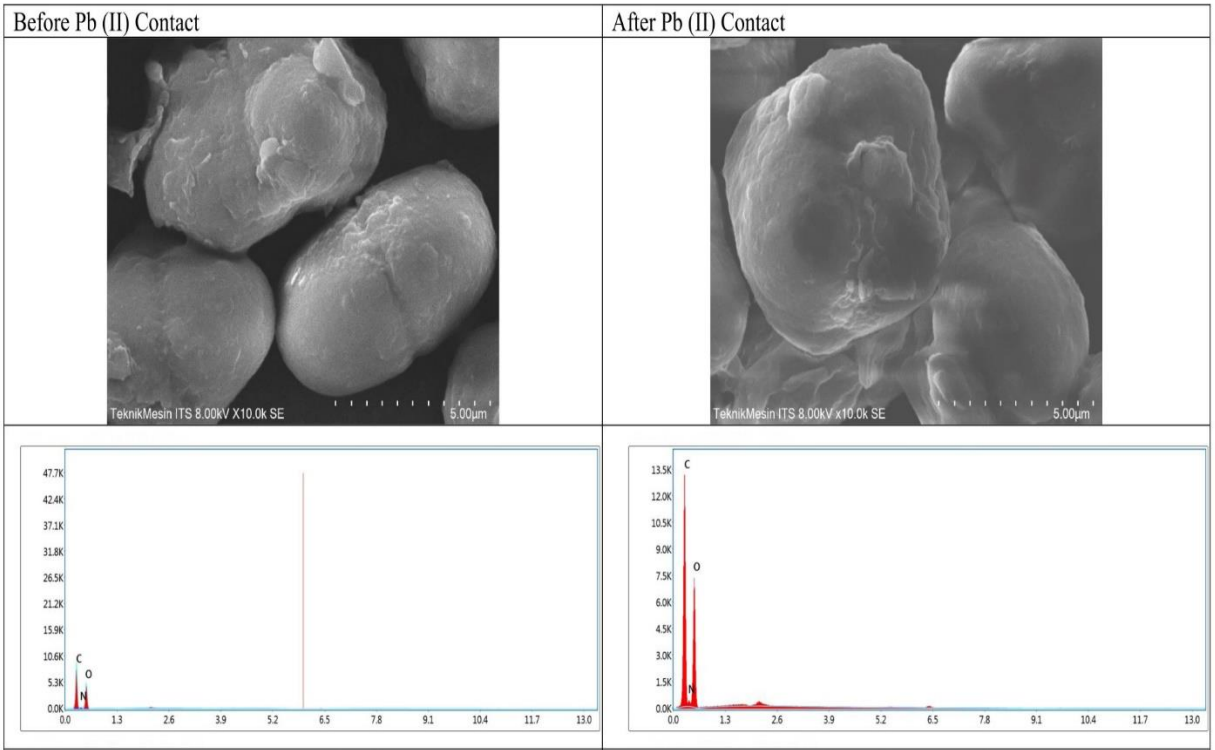

Smart Quant Result

Element	Weight (%)	Atomic (%)	Net Intensity	Error (%)	K-ratio
C (K)	45.82	52.63	494.57	5.60	0.2697
N (K)	5.19	5.12	13.78	15.62	0.0059
O (K)	48.99	42.25	307.69	9.73	0.0857

Smart Quant Result

Element	Weight (%)	Atomic (%)	Net Intensity	Error (%)	K-ratio
C (K)	46.94	53.74	755.91	5.43	0.2794
N (K)	5.45	5.35	20.88	13.81	0.0061
O (K)	47.60	40.91	429.21	9.66	0.0810

Figure 8. SEM–EDX analysis of the biosorbent before and after Pb(II) adsorption

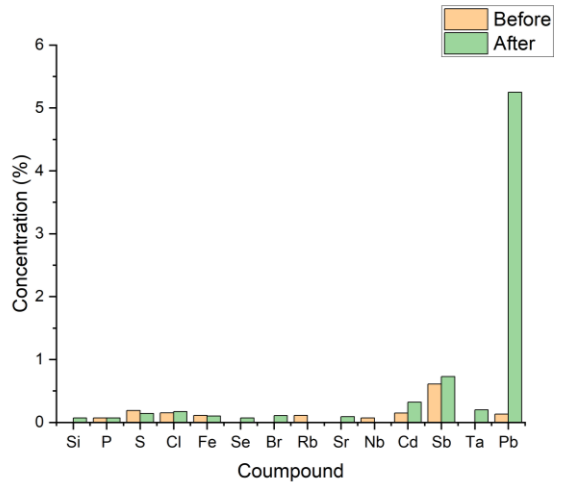

Figure 9. XRF analysis of the biosorbent before and after Pb(II) exposure

these demonstrate that SEM-EDX is an effective technique for analyzing the adsorption of heavy metals, such as Pb(II), onto various adsorbent materials.

XRF analysis

Figure 9 shows that the XRF results reveal substantial changes in elemental composition after the biosorbent comes into contact with Pb. The most notable change is the sharp increase in Pb content from 0.130% to 5.250%, which confirms strong interaction and accumulation of Pb(II) ions on the biosorbent surface. In addition to Pb, variations in the concentrations of other heavy metals such as Cd, Sb, Se, and Sr were also detected, suggesting active competitive adsorption among multiple ions. This behavior indicates that metals with a higher affinity for the biosorbent surface are preferentially retained.

These observations are consistent with those of [27,28]. It has been reported that advanced nanomaterials exhibit selective adsorption toward Pb(II) due to their tailored surface properties. Similar conclusions were drawn by [29,30], who found that the physicochemical characteristics of both the adsorbent and the surrounding medium strongly govern competitive adsorption among heavy metals. Collectively, these studies reinforce the notion that differences in surface functionality and affinity significantly influence the adsorption efficiency of various heavy metal ions.

RSM-BBD of analysis

The optimization of adsorption conditions was performed using RSM combined with a BBD. RSM is a statistical and mathematical approach that employs polynomial models to describe system behavior, allowing simultaneous evaluation and optimization of multiple operational variables. The BBD framework, in particular, is widely regarded as an efficient and cost-effective design strategy for optimizing chemical and physical processes. In this work, solution pH, initial Pb(II) concentration, and contact time were selected as the independent factors, while adsorption capacity (mg/g) served as the response variable. A total of 16 experimental runs were generated according to a three-factor, three-level BBD matrix and evaluated using Design Expert version 13.

The optimized conditions for Pb(II) removal using matoa seed powder were determined to be pH 6, an initial concentration of 600 mg/L, and a contact time of 60 min, yielding a maximum adsorption capacity of 74 mg/g. The empirical model produced through RSM provides a predictive tool for estimating Pb(II) removal efficiency under various operational scenarios. Analysis of Variance (ANOVA) results indicated that the initial concentration (B) and the quadratic effect of contact time (C^2) were statistically significant factors influencing the adsorption process.

Equation 3 in actual factor form from the RSM analysis is written as follows:

Adsorption capacity (q) = -644.79 + 42.29A + 1.51B + 2.84C - 0.021A·B + 0.0887A·C - 0.0028B·C - 2.40A^2 - 0.00093B^2 - 0.014C^2 (3)

Where, A = solution pH, B = initial Pb(II) concentration (mg/L), and C = contact time (min).

This regression equation allows the prediction of the response (adsorption capacity) for any combination of input variables within the experimental range. Although the overall model did not reach statistical significance ($p > 0.05$), the plot comparing predicted versus actual values demonstrated a reasonably good agreement, with only minor deviations. This indicates that the RSM–BBD framework continues to provide meaningful predictive capability and remains a practical tool for assessing and optimizing Pb(II) biosorption conditions.

These results are consistent with several earlier studies utilizing the RSM–BBD approach for heavy metal adsorption. Ighalo and Eletta showed that the biosorption of Pb(II) and Zn(II) using *Micropogonias undulatus* fish scales was optimized, achieving a removal efficiency of 98.76% with a model exhibiting an R^2 value of 0.89, indicating strong predictive strength [31]. Similarly, Okolo *et al*. evaluated biosorbents derived from African elemi and Mucuna seed husks, achieving an efficiency of 99.6% under optimized conditions with an excellent model fit (R^2 = 0.996) [32]. In addition, Ni'mah *et al.* developed a silica-based gel biosorbent from recycled glass bottle waste. They reported a Pb(II) removal efficiency of 99.77%, supported by an accurate RSM–BBD model [33]. Collectively, these comparisons underscore the reliability of the RSM–BBD methodology across various biosorption systems and reinforce its suitability for optimizing heavy metal removal processes.

Table 2 summarizes the comparison between the actual and predicted adsorption capacities, along with several diagnostic statistics, including residuals, studentized residuals, and Difference in Fits (DFFITS) values. Runs 2 and 13 show notably high residuals (>11 mg/g) and substantial DFFITS values (>8), suggesting that these data points act as influential outliers that disproportionately affect the model's behavior. Such deviations may arise from experimental inconsistency or reflect extreme operating conditions that the quadratic model does not adequately represent. In contrast, most of the remaining experimental runs exhibit relatively small residuals and low influence statistics, indicating that the model successfully describes the general response pattern.

These findings are in agreement with the ANOVA results, which produced a model p-value of 0.135, slightly above the commonly accepted threshold for statistical significance. Despite this, the close correspondence between predicted and experimental values, particularly near the optimal operating conditions (pH 6, initial concentration 600 mg/L, and contact time 60 min), indicates that the model retains sufficient predictive capability for practical use. Similar trends have been documented in earlier studies. For example, optimized Pb(II) adsorption using an MnO_2/MgFe LDO composite via RSM and achieved a maximum capacity of 531.86 mg/g, with R^2 values exceeding 0.998, demonstrating excellent model accuracy [34]. Likewise, RSM was applied to evaluate Pb(II) and Cd(II) uptake by modified coconut shell biochar, reporting similarly high R^2 values that confirm the methodology's robustness for developing waste-derived adsorbents [35]. In another example, Gholamiyan *et al.* used RSM to optimize erythromycin removal with magnetic activated carbon, achieving a 96.2% removal efficiency and observing strong agreement between the model predictions and experimental outcomes.

Table 2. Summary of analysis results using RSM–BBD

Run order	Actual value	Predicted value	Residual	Leverage	Studentized residual	DFFITS
1.0	72.631	67.614	5.017	0.75	0.99	1.719
2.0	37.538	26.352	11.185	0.75	2.22	8.22
3.0	60.12	66.097	-5.978	0.75	-0.68	-0.375
4.0	69.1	66.097	3.002	0.75	0.34	0.183
5.0	50.96	42.429	8.531	0.75	1.69	3.692
6.0	65.26	61.746	3.514	0.75	0.7	1.148
7.0	31.863	36.879	-5.017	0.75	-0.99	-1.719
8.0	50.706	53.36	-2.654	0.75	-0.53	-0.851
9.0	41.36	47.528	-6.168	0.75	-1.22	-2.229
10.0	62.288	59.633	2.654	0.75	0.53	0.851
11.0	39.95	43.464	-3.514	0.75	-0.7	-1.148
12.0	66.15	59.982	6.168	0.75	1.22	2.229
13.0	33.894	45.079	-11.185	0.25	-2.22	-8.22
14.0	45.906	54.437	-8.531	0.25	-1.69	-3.692
15.0	66.76	66.097	0.662	0.25	0.08	0.04
16.0	68.41	66.097	2.312	0.25	0.26	0.14

Collectively, these comparisons support the reliability of the RSM–BBD approach in optimizing adsorption systems, even when datasets include influential points or experimental variability [36]. To further improve model accuracy and strengthen statistical significance, the replication of outlier runs and stricter control over experimental parameters are recommended.

Parametric analysis of Pb(II) biosorption performance

Figure 10 illustrates the three response surface plots that depict how the principal variables interact during Pb(II) biosorption onto matoa seed powder. In plot (a), which evaluates the combined effects of solution pH and initial Pb(II) concentration, adsorption capacity rises substantially and peaks at approximately pH 6.0–6.5 and 650–700 mg/L Pb(II), consistent with the optimum conditions predicted by the RSM model.

Plot (b), which maps the interaction between pH and contact time, indicates that the maximum adsorption performance occurs at approximately pH 6.0 with contact times between 60 min and 75 min. Beyond this range, adsorption capacity stabilizes, indicating that the system has approached equilibrium. In plot (c), the combined influence of high initial Pb(II) concentration (around 700 mg/L) and a moderate contact time (around 60 min) highlights the most favorable conditions for Pb(II) uptake. These results corroborate experimental findings showing that the biosorbent achieves a maximum adsorption capacity of 74 mg/g under these optimized settings. Taken together, the three quadratic response surfaces affirm the reliability of the RSM model, clearly emphasizing the significance of the initial concentration (B) and the quadratic contact time term (C^2) as identified through ANOVA. These modeling results are strongly supported by complementary characterization

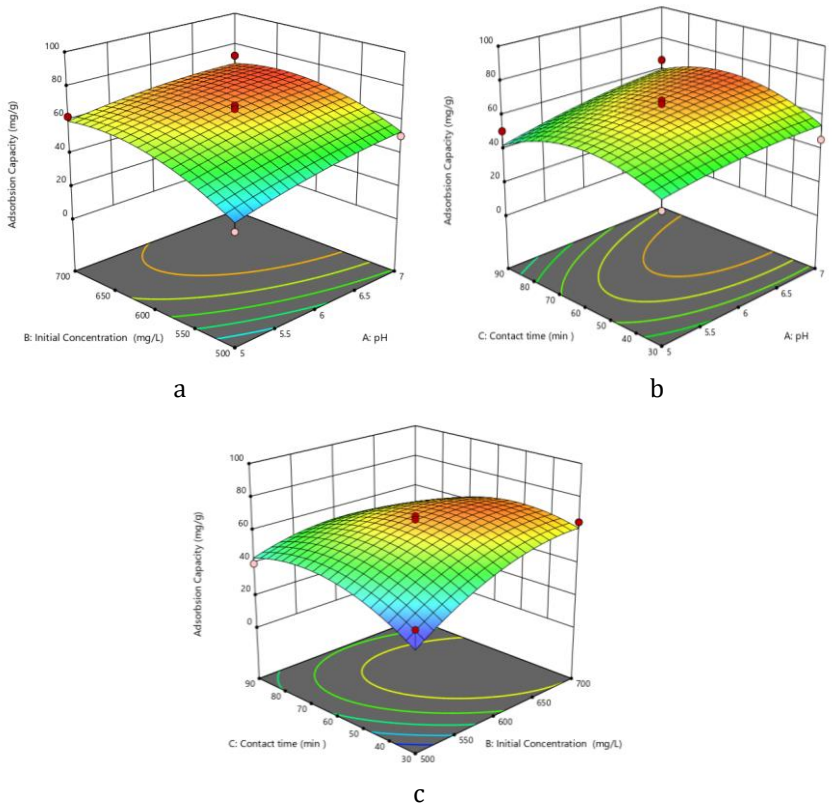

Figure 10. Response surface plot for adsorption of metal Pb (a. pH vs. initial concentration; b. pH vs. contact time; and c. contact time vs. initial concentration)

analyses: FTIR spectra reveal shifts in hydroxyl and carbonyl functional groups after Pb(II) adsorption, BET measurements show that the pore structure of the biosorbent remains largely intact, and XRF coupled with SEM–EDX confirms substantial Pb accumulation on the material—reaching up to 5.25 wt%. The relevance of these findings is further supported by comparison with previous studies. Abioye *et al.* successfully utilized RSM–BBD to optimize Pb(II) biosorption using *Saccharomyces cerevisiae* and *Candida tropicalis*, achieving removal efficiencies exceeding 94% at a pH of 5 and a contact time of 60 min [37]. Likewise, Ighalo and Eletta reported removal efficiencies above 98% when employing fish scale biomass as an adsorbent, with strong model agreement (R^2 = 0.89) within a pH range of 4–5 [31]. Collectively, these results demonstrated that the matoa seed powder biosorption system, when optimized through the RSM–BBD methodology, exhibited consistent, predictable, and scientifically reliable performance for Pb(II) removal from aqueous solutions.

Comparison study of matoa seed with literature

The performance of the activated *Pometia pinnata* (matoa seed) biosorbent obtained in this study was compared to various adsorbents reported in recent literature, as shown in Table 3. The adsorption capacity achieved here (74 mg/g) surpassed that of several natural biosorbents, including *Brassica nigra* biomass (7.2 mg/g) [38] and a range of agricultural by-products (45–50 mg/g) [39]. Although synthetic

materials, such as modified reduced graphene oxide (m-RGO), exhibit exceptionally high capacities (≈858 mg/g) [40], their preparation typically requires costly chemical treatments, raising sustainability concerns. In contrast, the matoa seed–derived biosorbent offers a practical compromise between adsorption efficiency and environmental compatibility, making it a promising candidate for real-world wastewater treatment. Regarding operational conditions, the optimal pH of 6 and equilibrium time of 60 min observed in this study are more favorable compared to many biosorbents that require strongly acidic environments (pH 3–5) or longer contact periods (90–120 min). Similar near-neutral pH performance was reported by [41] for EPS produced by *Klebsiella* sp. J1, which achieved a slightly higher adsorption capacity (99.5 mg/g) but only under relatively low initial Pb(II) concentrations (20 mg/L), suggesting limited applicability for systems with higher pollutant loads. Additionally, unlike numerous previous studies that relied on traditional batch experiments or one-factor-at-a-time (OFAT) methods, the present research employed response surface methodology (RSM) using a Box–Behnken Design (BBD) to refine adsorption conditions.

Table 3. Comparison of matoa seed biosorbent with other adsorbent materials

No.	Adsorbent	Heavy metal type	Adsorption capacity (mg/g)	Method / Technique	Optimum pH	Contact time (min)	Initial concentration (Co) (mg/L)	Ref.
1	Activated matoa seed (*Pometia pinnata*)	Pb(II)	74	RSM – Box–Behnken Design	6	60 min	600 mg/L	Present study
2	SR–PAA hydrogel from soybean residue	Pb(II) & Cd (II)	-	Hydrogel from waste biomass; batch	6	-	-	[14]
3	New Pb (II) adsorption study	Pb(II)	48.75 mg/g (Langmuir q_m reported)	Applied methods & modelling (FFNN	4	60	100	[30]
4	B. nigra biosorbent	Pb(II)	7.2 (Maximum)	Batch biosorption	4–5	605 min	30 mg/L	[38]
5	Agricultural residue-based biosorbent	Pb(II)	45–50	Batch adsorption	5	90	100	[39]

No.	Adsorbent	Heavy metal type	Adsorption capacity (mg/g)	Method / Technique	Optimum pH	Contact time (min)	Initial concentration (Co) (mg/L)	Ref.
6	Modified reduced graphene oxide (m-RGO)	Pb(II)	858	Carbon nanosheet adsorption	7	(Not specified)	(Not specified)	[40]
7	EPS from *Klebsiella sp. J1*	Pb(II)	99.5	Batch biosorption	6	(Equilibration time)	20 mg/L	[41]
8	Peanut shell, wood dust, activated carbon	Pb(II), Cu(II), and Cd(II)	(Varied)	Comparative batch adsorption	5–7	10–1,440 min	20–400 mg/L	[42]
9	Various biosorbents	Pb(II)	(Varied)	Batch + parametric optimization	(Varied)	(Varied)	(Varied)	[43]
10	Lycium barbarum branch	Pb(II), Cd(II), and Zn(II)	(Varied per metal)	Batch adsorption	(Varied)	(Varied)	(Varied)	[44]
11	Plant waste biosorbent	Pb(II)	(Reported in the study)	Batch biosorption	(Varied)	(Varied)	(Varied)	[45]
12	MGO@CA (magnetic graphene-oxide / calcium-alginate composite)	Pb(II)	270.27	Magnetic GO-alginate composite; batch; isotherm & kinetics; regenerable.	6	-	-	[46]
13	Acidic-group modified biochar (AMBC)	Pb(II)	148.6	Functionalised biochar; batch isotherm & kinetics.	5	30–120	100	[47]

No.	Adsorbent	Heavy metal type	Adsorption capacity (mg/g)	Method / Technique	Optimum pH	Contact time (min)	Initial concentration (Co) (mg/L)	Ref.
14	Waste-based carbon adsorbent (Cd study example)	Cd(II)	(Reported high removal; example system: q not comparable)	Waste carbon; batch	5	30	120	[48]
15	Ca-CHM / modified lignite (acid mine drainage context)	Pb(II) and Cd(II)	Pb q range 14.45–30.68	Modified coal/lignite materials; batch	4	-	-	[49]
16	Polymeric/ composite adsorbent)	Pb(II) and Cu(II)	48.75	Polymer/ composite; batch experiment	Range tested 2–6;	5–150	-	[50]
17	Fast adsorbent (example: nanosorbent)	Pb(II)	Reported fast uptake; equilibrium (high % in seconds)	Nano-adsorbent; batch	5	1,440	200	[51]
18	Perovskite /oxide composite study	Pb(II), Cd(II), and Cu(II)	Capacities reported per metal (see paper)	Composite inorganic adsorbents; batch	7	120	-	[52]
19	Review with data table (nanoadsorbents)	Various heavy metals	Lists q ranges and optimums (example: optimum pH ~9 for some nano)	Overview of nano-adsorbents and their optima	6.8 to Cu 7.3 to Zn	120	-	[53]
20	(Fixed-bed / column studies) cellulose-g-HAP	Pb(II) Cu(II)	Pb 59.6 mg/g (column mode reported)	Fixed-bed granules; column tests	6	30	Co range 10 – 50 $mg \cdot L^{-1}$ (column tests)	[54]

This multivariate optimization approach provides deeper insight into variable interactions and yields a statistically verified predictive model; an advantage not commonly explored in earlier biosorption investigations.

Conclusion

The results indicate that acid activated matoa seeds (*Pometia pinnata*) powder is an attractive, inexpensive, and sustainable biosorbent for removing Pb(II) from aqueous systems. Through

optimization using response surface methodology with a Box–Behnken Design, the optimal operational conditions were identified as pH 6, an initial Pb(II) concentration of 600 mg/L, and a contact time of 60 min, yielding a maximum adsorption capacity of 74 mg/g. FTIR characterization revealed that hydroxyl and carbonyl functional groups play a significant role in the interaction with Pb(II). At the same time, SEM–EDX and XRF analyses revealed distinct surface modifications and elevated Pb levels on the biosorbent following adsorption. The successful application of RSM underscores its usefulness as a predictive and optimization tool for biosorption processes. Overall, the results validate matoa seed powder as an efficient and sustainable adsorbent suitable for treating wastewater contaminated with heavy metals.

Acknowledgements

The author would like to thank Andalas University for its support in completing this research under contract number 060/C3/DT.05.00/PL/2025.

Conflict of Interest

The authors declare that there is no conflict of interest regarding the publication of this manuscript. In addition, the authors have completely observed the ethical issues; including plagiarism, informed consent, misconduct, data fabrication and/ or falsification, double publication and/or submission, and redundancy.

ORCID

Arief Yandra Putra
https://orcid.org/0009-0005-4728-050X
Safni Safni
https://orcid.org/0000-0003-0307-5211
Rahmiana Zein
https://orcid.org/0000-0002-4281-2993
Emriadi Emriadi
https://orcid.org/0000-0001-9915-1930

References

[1] Ameen, M.M., Moustafa, A.A., Mofeed, J., Hasnaoui, M., Olanrewaju, O.S., Lazzaro, U., Guerriero, G., Factors affecting efficiency of biosorption of Fe(III) and Zn(II) by ulva lactuca and corallina officinalis and their activated carbons. *Water*, **2021**, 13(23), 3421.
[2] Zein, R., Tomi, Z.B., Fauzia, S., Zilfa, Z. Modification of rice husk silica with bovine serum albumin (bsa) for improvement in adsorption of metanil yellow dye. *Journal of the Iranian Chemical Society*, **2020**, 17(10), 2599-2612.
[3] Kriswandana, F., Winarko, W. The effectiveness of reduction of weight metal contents of pb, and hg in water electro-coagulation method. *Journal of Global Pharma Technology*, **2020**, 306-313.
[4] Alabi, O., Olanrewaju, A.A., Afolabi, T.J. Process optimization of adsorption of Cr (VI) on adsorbent prepared from bauhinia rufescens pod by box-behnken design. *Separation Science and Technology*, **2020**, 55(1), 47-60.
[5] Hevira, L., Ighalo, J.O., Zein, R. Biosorption of indigo carmine from aqueous solution by terminalia catappa shell. *Journal of Environmental Chemical Engineering*, **2020**, 8(5), 104290.
[6] Ren, G., Jin, Y., Zhang, C., Gu, H., Qu, J. Characteristics of bacillus sp. Pz-1 and its biosorption to Pb(II). *Ecotoxicology and Environmental Safety*, **2015**, 117, 141-148.
[7] Ali Redha, A. Removal of heavy metals from aqueous media by biosorption. *Arab Journal of Basic and Applied Sciences*, **2020**, 27(1), 183-193.
[8] Zulfahmi, Z., Pertiwi, S.A., Rosmaina, R., Elfianis, R., Gulnar, Z., Zhaxybay, T., Bekzat, M., Zhaparkulova, G. Molecular identification of mother trees of four matoa cultivars (*Pometia pinnata* forst & forst) from pekanbaru city, indonesia using rapd markers. *Biodiversitas Journal of Biological Diversity*, **2023**, 24(3), 1524–1529.
[9] Sihotang, Y.M., Windiasfira, E., Barus, H.D.G., Herlina, H., Novita, R.P. Hepatoprotective effect of ethanol extract of matoa leaves (*Pometia pinnata*) against paracetamol-induced liver disease in rats. *Science and Technology Indonesia*, **2017**, 2(4), 92-95.
[10] Kustomo, K., Faza, N.L.Z., Haarstrick, A. Adsorption of Cd(II) into activated charcoal from matoa fruit peel. *Walisongo Journal of Chemistry*, **2022**, 5(1), 83-93.
[11] Fauzia, S., Aziz, H., Dahlan, D., Namieśnik, J., Zein, R. Adsorption of Cr (VI) in aqueous solution using sago bark (metroxylon sagu) as a new potential

biosorbent. *Desalination and Water Treatment*, **2019**, 147, 191-202.
[12] Putra, A., Fauzia, S., Arief, S., Zein, R. Preparation, characterization, and adsorption performance of activated rice straw as a bioadsorbent for Cr (VI) removal from aqueous solution using a batch method. *Desalination and Water Treatment*, **2022**, 264, 121-132.
[13] Mashentseva, A.A., Seitzhapar, N., Barsbay, M., Aimanova, N.A., Alimkhanova, A.N., Zheltov, D.A., Zhumabayev, A.M., Temirgaziev, B.S., Almanov, A.A., Sadyrbekov, D.T. Adsorption isotherms and kinetics for Pb(II) ion removal from aqueous solutions with biogenic metal oxide nanoparticles. *RSC Advances*, **2023**, 13(38), 26839-26850.
[14] Zhang, M., Yin, Q., Ji, X., Wang, F., Gao, X., Zhao, M. High and fast adsorption of Cd(II) and Pb(II) ions from aqueous solutions by a waste biomass-based hydrogel. *Scientific Reports*, **2020**, 10(1), 3285.
[15] Kalaiselvi, K., Mohandoss, S., Ahmad, N., Khan, M.R., Manoharan, R.K. Adsorption of Pb^{2+} ions from aqueous solution onto porous kappa-carrageenan/cellulose hydrogels: Isotherm and kinetics study. *Sustainability*, **2023**, 15(12), 9534.
[16] Esmaeili, A., Eslami, H. Adsorption of Pb(II) and Zn(II) ions from aqueous solutions by red earth. *MethodsX*, **2020**, 7, 100804.
[17] Ali, A., Alharthi, S., Ahmad, B., Naz, A., Khan, I., Mabood, F. Efficient removal of Pb(II) from aqueous medium using chemically modified silica monolith. *Molecules*, **2021**, 26(22), 6885.
[18] Sari, M.K., Basuki, R., Rusdiarso, B. Adsorption of Pb(II) from aqueous solutions onto humic acid modified by urea-formaldehyde: Effect of ph, ionic strength, contact time, and initial concentration. *Indonesian Journal of Chemistry*, **2021**, 21(6), 1371-1388.
[19] Chowdhury, T., Zhang, L., Zhang, J., Aggarwal, S. Pb(II) adsorption from aqueous solution by an aluminum-based metal organic framework–graphene oxide nanocomposite. *Materials Advances*, **2021**, 2(9), 3051-3059.
[20] Yang, Y., Sun, F., Li, J., Chen, J., Tang, M. The effects of different factors on the removal mechanism of Pb(II) by biochar-supported carbon nanotube composites. *RSC Advances*, **2020**, 10(10), 5988-5995.
[21] Li, Y., Peng, L., Li, W. Adsorption behaviors on trace Pb^{2+} from water of biochar adsorbents from konjac starch. *Adsorption Science & Technology*, **2020**, 38(9-10), 344-356.
[22] Tang, S.F., Zhou, H., Tan, W.T., Huang, J.G., Zeng, P., Gu, J.F., Liao, B.H. Adsorption characteristics and mechanisms of Fe-Mn oxide modified biochar for Pb(II) in wastewater. *International Journal of Environmental Research and Public Health*, **2022**, 19(14), 8420.
[23] Chen, J., Duan, Q., Liu, J., Zhang, S., Zhang, J., Lin, S. Adsorption of Fe-modified peanut shell biochar for Pb(II) in mixed Pb(II), Cu(II), Ni(II) solutions. *Scientific Reports*, **2025**, 15(1), 13558.
[24] Bai, T., Zhao, J., Tian, L., Zhang, L., Jin, Z. The adsorption of Pb(II) from aqueous solution using koh-modified banana peel hydrothermal carbon: Adsorption properties and mechanistic studies. *Materials*, **2024**, 17(2).
[25] Khater, D., Alkhabbas, M., Al-Ma'abreh, A.M. Adsorption of Pb, Cu, and ni ions on activated carbon prepared from oak cupules: Kinetics and thermodynamics studies. *Molecules*, **2024**, 29(11), 2489.
[26] Kaur, M., Kumari, S., Sharma, P. Removal of Pb(II) from aqueous solution using nanoadsorbent of oryza sativa husk: Isotherm, kinetic and thermodynamic studies. *Biotechnology Reports*, **2020**, 25, e00410.
[27] Tang, D., Zhang, Q., Tan, G., He, L., Xia, F. Retracted: Adsorption capability and mechanism of Pb(II) using MgO nanomaterials synthesized by ultrasonic electrodeposition. *Coatings*, **2024**, 14(7), 891.
[28] Deng, H., Zhang, S., Li, Q., Li, A., Gan, W., Hu, L. Efficient removal of lead, cadmium, and zinc from water and soil by mgfe layered double hydroxide: Adsorption properties and mechanisms. *Sustainability*, **2024**, 16(24), 11037.
[29] Fan, D., Peng, Y., He, X., Ouyang, J., Fu, L., Yang, H. Recent progress on the adsorption of heavy metal ions Pb(II) and Cu(II) from wastewater. *Nanomaterials*, **2024**, 14(12), 1037.
[30] Abd El-wahaab, B., El-Shwiniy, W.H., Alrowais, R., Nasef, B.M., Said, N. Adsorption of lead (Pb(II)) from contaminated water onto activated carbon: Kinetics, isotherms, thermodynamics, and modeling by artificial intelligence. *Sustainability*, **2025**, 17(5), 2131.
[31] Ighalo, J.O., Eletta, O.A. Response surface modelling of the biosorption of Zn(II) and Pb(II) onto micropogonias undulatus scales: Box–behnken experimental approach. *Applied Water Science*, **2020**, 10(8), 1-12.
[32] Okolo, B.I., Oke, E., Agu, C.M., Adeyi, O., Nwoso-Obieogu, K., Akatobi, K. Adsorption of lead (II) from aqueous solution using africa elemi seed, mucuna shell and oyster shell as adsorbents and optimization using box–behnken design. *Applied Water Science*, **2020**, 10(8), 1-23.
[33] Ni'mah, Y., Yuningsih, N., Suprapto, S. The adsorption of Pb(II) using silica gel synthesized from chemical bottle waste: Optimization using box-

behnken design. *Journal of Renewable Materials*, **2023**, 11(6), 2913.
[34] Huang, Y., Luo, X., Liu, C., You, S., Rad, S., Qin, L. Effective adsorption of Pb(II) from wastewater using MnO 2 loaded MgFe-Ld (h) o composites: Adsorption behavior and mechanism. *RSC Advances*, **2023**, 13(28), 19288-19300.
[35] Qin, H., Shao, X., Shaghaleh, H., Gao, W., Hamoud, Y.A. Adsorption of Pb^{2+} and Cd^{2+} in agricultural water by potassium permanganate and nitric acid-modified coconut shell biochar. *Agronomy*, **2023**, 13(7), 1813.
[36] Gholamiyan, S., Hamzehloo, M., Farrokhnia, A. RSM optimized adsorptive removal of erythromycin using magnetic activated carbon: Adsorption isotherm, kinetic modeling and thermodynamic studies. *Sustainable Chemistry and Pharmacy*, **2020**, 17, 100309.
[37] Abioye, O.P., Usman, A., Oyewole, O.A., Aransiola, S.A. Application of box-behnken model to study biosorption of lead by saccharomyces cerevisiae and candida tropicalis isolated from electrical and electronic waste dumpsite. *Global NEST Journal*, **2020**, 22, 1,95-101.
[38] Reátegui-Romero, W., Cadenas-Vásquez, W.J., King-Santos, M.E., Alvarez, W.F.Z., Posadas, R.A. Evaluation of Pb(II) adsorption from aqueous solutions using brassica nigra as a biosorbent. *The Open Biotechnology Journal*, **2019**, 13(1).
[39] Putra, A., Elsa Fitri, W., Yuniko, F., Handayani, T., Hidayat, H., Ighalo, J.O. Evaluating the potential of duck egg shell for methylene blue adsorption in medical laboratory wastewater. *Pollution*, **2025**, 11(3), 828-845.
[40] Kim, H.G., Bae, J.S., Hwang, I., Kim, S.H., Jeon, K.W. Superior heavy metal ion adsorption capacity in aqueous solution by high-density thiol-functionalized reduced graphene oxides. *Molecules*, **2023**, 28(10), 3998.
[41] Wei, W., Wang, Q., Li, A., Yang, J., Ma, F., Pi, S., Wu, D. Biosorption of Pb(II) from aqueous solution by extracellular polymeric substances extracted from klebsiella SP. J1: Adsorption behavior and mechanism assessment. *Scientific reports*, **2016**, 6(1), 31575.
[42] Devi, B., Goswami, M., Rabha, S., Kalita, S., Sarma, H.P., Devi, A. Efficacious sorption capacities for Pb (II) from contaminated water: A comparative study using biowaste and its activated carbon as potential adsorbents. *ACS Omega*, **2023**, 8(17), 15141-15151.
[43] Li, J., Dong, X., Liu, X., Xu, X., Duan, W., Park, J., Gao, L., Lu, Y. Comparative study on the adsorption characteristics of heavy metal ions by activated carbon and selected natural adsorbents. *Sustainability*, **2022**, 14(23), 15579.
[44] Guan, J., Hu, C., Zhou, J., Huang, Q., Liu, J. Adsorption of heavy metals by lycium barbarum branch-based adsorbents: Raw, fungal modification, and biochar. *Water Science and Technology*, **2022**, 85(7), 2145-2160.
[45] Kirova, G., Velkova, Z., Stoytcheva, M., Hristova, Y., Iliev, I., Gochev, V. Biosorption of Pb(II) ions from aqueous solutions by waste biomass of streptomyces fradiae pretreated with naoh. *Biotechnology & Biotechnological Equipment*, **2015**, 29(4), 689-695.
[46] Malitha, S.B., Mahmudunnabi, D.M., Mazumder, S., Hossain, K.S., Nurnabi, M., Alam, M.Z. Rapid adsorptive removal of Pb $^{2+}$ ions from aqueous systems using a magnetic graphene oxide calcium alginate composite: Optimisation, isotherms, and kinetics. *Environmental Science: Advances*, **2025**, 4(4), 595-605.
[47] Wu, Y., Li, C., Wang, Z., Li, F., Li, J., Xue, W., Zhao, X. Enhanced adsorption of aqueous Pb(II) by acidic group-modified biochar derived from peanut shells. *Water*, **2024**, 16(13), 1871.
[48] Gelaw, Y.B., Dagne, H., Adane, B., Yirdaw, G., Moges, M., Aneley, Z., Kumlachew, L., Aschale, A., Deml, Y.A., Tegegne, E. Adsorptive removal of cadmium (II) from wastewater using activated carbon synthesized from stem of khat (catha edulis). *Heliyon*, **2024**, 10(22).
[49] An, W., Liu, Y., Chen, H., Sun, X., Wang, Q., Hu, X., Di, J. Adsorption properties of Pb (II) and Cd (II) in acid mine drainage by oyster shell loaded lignite composite in different morphologies. *Scientific Reports*, **2024**, 14(1), 11627.
[50] Kandil, H., El-Wakeel, S.T. Effective removal of Pb(II) and Cu (II) from aqueous solutions using a hybrid composite of fuller's earth, aluminum silicate and chitosan. *Polymer Bulletin*, **2024**, 81(2), 1839-1859.
[51] XXia, Y., Li, Y., Xu, Y. Adsorption of Pb (II) and Cr (VI) from aqueous solution by synthetic allophane suspension: Isotherm, kinetics, and mechanisms. *Toxics*, **2022**, 10(6), 291.
[52] Ali, S.M., El Mansop, M.A., Galal, A., Abd El Wahab, S.M., El-Etr, W.M., Zein El-Abdeen, H.A. A correlation of the adsorption capacity of perovskite/biochar composite with the metal ion characteristics. *Scientific Reports*, **2023**, 13(1), 9466.
[53] Deliza, D., Safni, S., Zein, R., Putri, R.A. Bio-inspired TiO_2 nanoparticles: green photocatalysts for azo dyes driven by UV-A. *Advanced Journal of Chemistry, Section A,* **2026**, 9(4), 610–625.
[54] Marrane, S.E., Dânoun, K., Essamlali, Y., Aboulhrouz, S., Sair, S., Amadine, O., Jioui, I., Rhihil, A., Zahouily, M. Fixed-bed adsorption of Pb(II) and Cu(II) from multi-metal aqueous systems onto cellulose-g-hydroxyapatite granules: Optimization using response surface methodology. *RSC Advances*, **2023**, 13(45), 31935-31947.

HOW TO CITE THIS MANUSCRIPT
A.Y. Putra, S. Safni, R. Zein, E. Emriadi. A Novel Biosorbent Derived from Matoa Seeds (*Pometia pinnata*) for Lead Removal: Optimization and Material Characterization. *Asian Journal of Green Chemistry*, 10 (4) 2026, 673-693.
DOI: https://doi.org/0.48309/ajgc.2026.566613.1892
URL: https://www.ajgreenchem.com/article_239741.html